

Fig 1. Renal function after the intravenous injection of low serum cultured human adipose tissue-derived stromal cells (hLASCs).

ischemia induced AKI¹⁾ and. Aim is to clarify the renoprotection of ASCs for ischemia induced AKI.

MATERIALS AND METHODS

Culture conditions

The basal culture medium was prepared as previously described⁴⁾.

In vivo experimental subcapsular administration of hASCs

Subcapsular injection of 2×10^6 of rat (r)-ASCs and control medium (Dulbecco's modified Eagle's medium, DMEM; Sigma-Aldrich) (each group n=6) was given to the left kidney of Acute kidney injury (AKI) rats. Blood samples were collected and blood urea nitrogen (BUN) and serum creatinine levels were measured by Mitsubishi Chemical Medience Co. Ltd (Tokyo, Japan). Rats were euthanized and renal cortical microcirculation was assessed using CCD video microscope³⁾ and kidney samples were taken for the study.

Morphological analysis

To evaluate tubulointerstitial injury, Hematoxylin Eosin (HE) and periodic acid Schiff (PAS) stained kidney sections were analysed using a quantitative grading.

Renal function

Rats treated with control medium demonstrated a marked rise in BUN and serum creatinine and, r-ASCs further suppressed the increase of serum creatinine (Figure 1).

Tubular injury

Examination of PAS stained kidney sections taken from AKI rats treated with control medium showed severe tubular cell degenerative changes with necrosis and luminal casts. A r-ASCs greatly attenuated the tubular injury. The severity of the tubular damage, including tubular dilatation, degeneration and cast formation was scored. Treatment with r-ASCs resulted in significantly better scores than the control. In contrast, the r-ASCs-treated group failed to show significantly better scores than the control group.

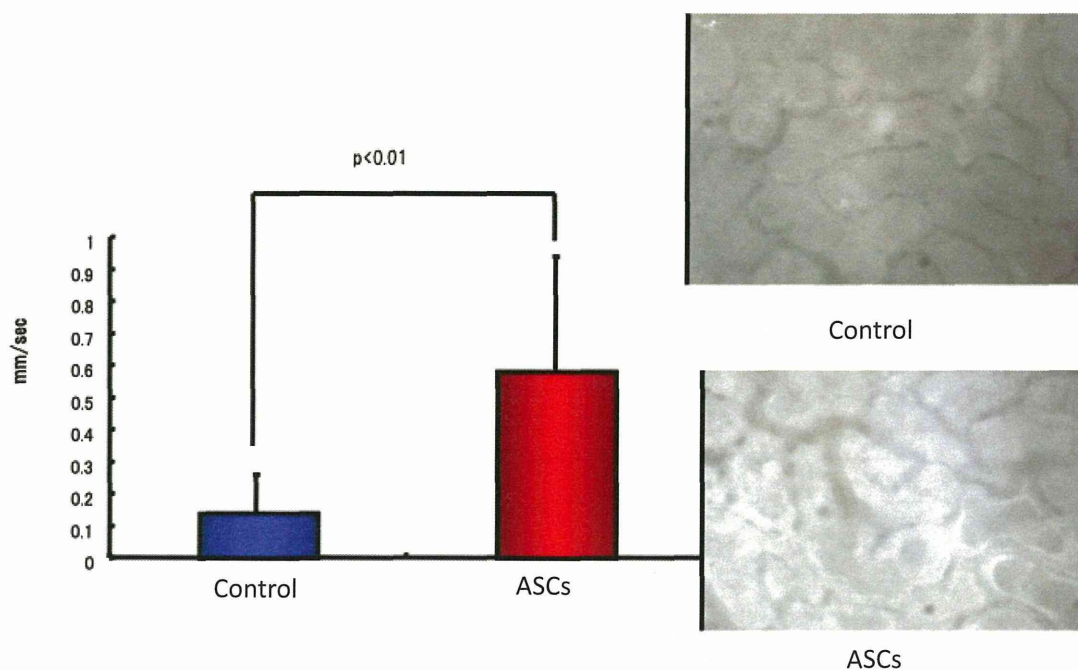


Fig 2. Renal cortical microcirculation. Velocity of the capillary blood flow and the capillary blood flow volume were significantly higher in AKI rats given subcapsular injection of hLASCs than those given the control medium.

Direct visualization of the renal cortical capillaries

The effects of r-ASCs on renal cortical microcirculation were examined by analyzing the direct images obtained with a CCD video microscope system. The blood flow velocity was significantly faster and the blood flow volume was greater in the r-ASCs group than in the control (Figure 2).

In conclusion, we demonstrate that subcapsular administration of r-ASCs protects the kidney via peritubular microcirculation from acute tubular injury.

References

- 1) Brodsky SV, Yamamoto T, Tada T, Kim B, Chen J, Kajiya F, Goligorsky MS. Endothelial dysfunction in ischemic acute renal failure: Rescue by transplanted endothelial cells. *Am J Physiol Renal Physiol* 2002;282:F1140-9.
- 2) Katsuno T, Ozaki T, Furuhashi K, Kim H, Yasuda K, Yamamoto T, Sato W, et al. Low serum cultured adipose tissue-derived stromal cells ameliorate acute kidney injury in rats. *Cell Transplantation* 2012 Sep 7. [Epub ahead of print]
- 3) Yamamoto T, Tada T, Brodsky SV, Tanaka H, Noiri E, Kajiya F, Goligorsky MS. Intravital videomicroscopy of peritubular capillaries in renal ischemia. *Am J Physiol Renal Physiol* 2002;282:F1150-5.
- 4) Iwashima S, Ozaki T, Maruyama S, Saka Y, Kobori M, Omae K, Yamaguchi H, et al. Novel culture system of mesenchymal stromal cells from human subcutaneous adipose tissue. *Stem Cells Dev* 2009;18(4):533-43.
- 5) Yasuda K, Ozaki T, Saka Y, Yamamoto T, Gotoh M, Ito Y, Yuzawa Y, Matsuo S, Maruyama S. Autologous cell therapy for cisplatin induced acute kidney injury by using non-expanded adipose tissue derived cells *Cytotherapy*. 2012 Oct;14(9):1089-100. doi: 10.3109/14653249.2012.693157. Epub 2012 Jun 25.

Autologous cell therapy for cisplatin-induced acute kidney injury by using non-expanded adipose tissue-derived cells

KAORU YASUDA¹, TAKENORI OZAKI¹, YOUSUKE SAKA¹, TOKUNORI YAMAMOTO², MOMOKAZU GOTOH², YASUHIKO ITO¹, YUKIO YUZAWA¹, SEIICHI MATSUI¹ & SHOICHI MARUYAMA¹

¹Department of Nephrology and ²Department of Urology, Nagoya University Graduate School of Medicine, Nagoya, Japan

Abstract

Background aims. Recent studies have demonstrated that cultured mesenchymal stromal cells derived from adipose tissue are useful for regenerative cell therapy. The stromal vascular fraction (SVF) can be obtained readily without culturing and may be clinically applicable. We investigated the therapeutic effects of SVF and used it in the treatment of acute kidney injury (AKI). **Methods.** Liposuction aspirates were obtained from healthy donors who had provided written informed consent. We harvested the SVF and determined the growth factor secretion and anti-apoptotic ability with conditioned medium. To investigate the effect of SVF on AKI, cisplatin was injected into rats and SVF was administered into the subcapsula of the kidney. **Results.** Both human and rat SVF cells secreted vascular endothelial growth factor-A (VEGF) and hepatocyte growth factor (HGF). Human SVF-conditioned media had an anti-apoptotic effect, which was inhibited by anti-HGF antibody (Ab) but not by anti-VEGF Ab. *In vivo*, SVF significantly ameliorated renal function, attenuated tubular damage and increased the cortical blood flow speed. In the SVF-treated group, VEGF levels in the cortex and HGF levels in both the cortex and medulla, especially tubules in the medulla, were significantly higher. Immunostaining revealed that SVF cells expressing VEGF and HGF and remained in the subcapsule on day 14. **Conclusions.** The present study demonstrates that a subcapsular injection of non-expanded SVF cells ameliorates rat AKI, and that the mechanism probably involves secretion of renoprotective molecules. Administration of human SVF may be clinically applicable and useful as a novel autologous cell therapy against kidney diseases.

Key Words: angiogenesis, growth factors, hepatocyte growth factor, implantation

Introduction

Accumulating evidence suggests that the adult body contains multipotent stem cells and/or progenitor cells that may be used for regenerative cell therapies on damaged organs (1–3). Animal and clinical studies have demonstrated that transplanted stem and progenitor cells obtained from bone marrow (BM) promote collateral formation of capillaries in ischemic tissues by differentiating into vascular cells and secreting angiogenic cytokines (4–6). Although BM aspiration can be applied in treating patients, it cannot be performed frequently because of its invasiveness. Moreover, cell culture may be needed to obtain a sufficient number of BM cells for use in human cell therapy. Early clinical trials have reported that the administration of a single angiogenic growth factor, such as vascular endothelial growth factor (VEGF)-A and hepatocyte growth factor (HGF), as a recombinant

protein or gene could enhance the formation of new collateral vessels, relieving some ischemic symptoms (7,8). As the efficacy and safety of current therapy is still controversial (9,10), an alternative source of stem/progenitor cells for regenerative therapy has long been sought.

Adipose tissues are reported to contain multipotent stem/progenitor cells that can promote regeneration of damaged organs (11,12). One of the main advantages of using fat as a source of stem/progenitor cells is that it can be obtained safely from subcutaneous tissue under local anesthesia. From fat, a cell population containing various types of immature cells is isolated after collagenase digestion and centrifugation. This cell population is called the stromal vascular fraction (SVF). Multicolor fluorescence-activated cell sorting (FACS) analysis has revealed that SVF are composed of heterogeneous cell populations

Correspondence: Dr Kaoru Yasuda, MD, PhD, Nagoya University Graduate School of Medicine, Department of Nephrology, Nagoya, Japan. E-mail: kyasuda@med.nagoya-u.ac.jp

(Received 23 October 2011; accepted 7 May 2012)

ISSN 1465-3249 print/ISSN 1477-2566 online © 2012 Informa Healthcare
DOI: 10.3109/14653249.2012.693157

including blood-derived cells, mesenchymal stromal/stem cells (MSC), endothelial (progenitor) cells and other cells. MSC is a major population, 15–40%, in SVF (13). MSC can be isolated and expanded from SVF, and many studies have shown the effectiveness of MSC when used for regenerative therapy (14). In a previous study, we have reported that MSC with high potential for regenerative cell therapy can be obtained from fat by a low-serum culture method (15). However, in order to obtain a sufficient number of MSC for use in cell therapy, culturing is necessary. This has limited the extent to which these cells could be used in human therapy. Previous studies have shown that SVF offers a sufficient number of stem/progenitor cells without culturing, and that non-expanded SVF cells can promote a tissue repair and regeneration of various organs (16–18). Therefore SVF is considered to be an attractive cell source for regenerative cell therapy, and several clinical studies demonstrating this have recently started.

Because little is known about the potential uses of SVF in diseases of the kidney, the present study aimed to examine the characteristics of SVF and investigated its therapeutic effects on acute kidney injury (AKI). This study demonstrates the usefulness of SVF in treating kidney diseases and presents data that allow immediate application to patients.

Methods

Human adipose tissue

Liposuction aspirates were obtained from nine healthy female donors who gave written informed consent and underwent liposuction of the abdomen or thighs. All tissue samples were used with approval and according to the guidelines of the ethical committee at the Nagoya University Medical School (approval number 505-2; Nagoya, Japan), and the study was performed according to the guidelines of the Declaration of Helsinki.

Animals

F344 male rats were purchased from CLER Inc. (Tokyo, Japan) and housed in accordance with the National Institutes of Health Guide for the Care and Use of Laboratory Animals. The protocols were approved by the Animal Care and Use Committee of Nagoya University.

Flow cytometry of SVF cells

Human (h)SVF was obtained from liposuction aspirates, and rat (r)SVF was obtained from the subcutaneous adipose tissue of F344 rats as described previously (11,14). Cell-surface markers

expressed on hSVF and rSVF cells were determined as described elsewhere (14). For the analysis of hSVF cells, antibodies (Ab) against the following cell-surface markers were used: phycoerythrin (PE)-conjugated Ab against CD13, CD90 or CD31, fluorescein isothiocyanate (FITC)-conjugated Ab against CD45, and allophycocyanin (APC)-conjugated Ab against CD34. All of these Ab were purchased from Becton Dickson (San Jose, CA, USA). For rSVF cells, Ab against CD31-PE, CD45-FITC (BD Biosciences, San Jose, CA, USA), CD34-FITC and CD13-FITC (Santa Cruz Biotechnology, Santa Cruz, CA) were also used. Flow cytometry was performed using a FACSVantage SE (BD Japan, Tokyo, Japan). All cells were stained with non-specific IgG to assess background fluorescence.

Cytokine secretion from hSVF and rSVF

hSVF cells (1×10^7) were placed on 10-cm tissue culture plates (Falcon BD Biosciences, Franklin Lakes, NJ, USA) in 10-mL Dulbecco's-modified Eagle medium (DMEM; Sigma, St Louis, MO, USA) containing 10% fetal bovine serum and incubated under either normoxic (21% O₂) or hypoxic (1% O₂) conditions for 24 h, and the conditioned media collected. The concentrations of VEGF and HGF were measured using commercial sandwich enzyme-linked immunosorbent assay (ELISA) kits: Quantikine human VEGF immunoassay (R&D Systems, Minneapolis, MN, USA) and HGF Otsuka ELISA (Otsuka Pharmaceutical Co., Tokyo, Japan).

Cytokine secretions from rSVF cells were measured with a similar method using commercial sandwich ELISA kits: rat VEGF assay and rat HGF enzyme immunoassay (EIA) (Institute of Immunology Co. Ltd, Tokyo, Japan). Rat adipose tissue-derived undifferentiated endothelial cells (RATEC) and MSC were cultured and their condition medium was also measured with cytokines in the same settings (15,19). RATEC were obtained from Dr Kitagawa, Nagoya University.

Cytoprotective activities of hSVF on tubular epithelial cells

The cytoprotective effects of hSVF cell-conditioned medium were evaluated using human renal proximal tubule epithelial cells (hRPTEC; Cambrex, Walkersville, MD, USA) as described elsewhere, with minor modifications (18). hRPTEC were cultivated in renal epithelial cell basal medium (REBM) supplemented with renal epithelial cells growth medium (REGM) SingleQuots (Cambrex) in 4-well chamber slides (Nalge Nunc International, Rochester, NY, USA) and

incubated for 24 h with cisplatin (25 μM) in the presence or absence of 50% conditioned medium obtained from hSVF. The culture media were collected, and the concentration of lactate dehydrogenase (LDH) was measured (Mitsubishi Chemical Medience Corporation, Tokyo, Japan). The cells were fixed with 4% paraformaldehyde in phosphate-buffered saline (PBS) and TdT-mediated dUTP nick end labeling, Takara (Osaka, Japan) (TUNEL) staining (apoptosis detection kit; Takara) was performed (19). Annexin V staining (Annexin V–fluorescein staining kit; Wako, Tokyo, Japan) was also performed, followed by flow cytometry.

The effects of VEGF and HGF secreted from hSVF cells on hRPTEC were examined by means of VEGF neutralizing goat polyclonal IgG (10 $\mu\text{g}/\text{mL}$; R&D Systems) and HGF neutralizing goat polyclonal IgG (10 $\mu\text{g}/\text{mL}$; R&D Systems) (14). A normal goat IgG fraction was used as a control. These neutralizing Ab and control were added to conditioned media with cisplatin, and Annexin V staining was performed.

Rat experimental protocol 1: subcapsular administration of rSVF

Eight-week-old male F344 rats ($n = 12$) were anesthetized with pentobarbital (50 mg/kg intraperitoneally; i.p.) and the right kidneys were removed. Seven days later (day 0), AKI was induced by subcutaneous (s.c.) injection of cisplatin (7 mg/kg). On day 1, 1×10^6 non-expanded SVF cells ($n = 6$) or saline ($n = 6$) were injected into the subcapsular space of the left kidney; 1-mL blood samples were collected on days 0, 2, 4, 8 and 14, and the levels of serum creatinine were measured using a Daiya Auto Crea kit (Daiya Shiyaku, Tokyo, Japan). At day 14, rats were anesthetized with pentobarbital (50 mg/kg i.p.), the blood flow speed measured, and the kidney removed for study. AKI was induced in another set of rats ($n = 12$) and rSVF or saline was injected into subcapsules of the kidney in a similar way. On day 6, rats were killed and kidney samples taken for study.

Renal cortical blood flow velocity

At day 14, the cortical capillary blood flow rate was measured using a pencil-probe videomicroscope with a charged-coupled device (CCD) camera system (20). The experimental system consisted of a specially ordered pencil-probe videomicroscope with a CCD camera (Nihon Kohden, Tokyo, Japan), micro-manipulator, light source (LA-60Me; Hayashi, Tokyo, Japan), monitor (PVM-146J; Sony, Tokyo, Japan), videocassette recorder (VCR; WV-ST1; Sony) and a computer for image analysis (Power Macintosh G3; Apple Computer, Cupertino, CA, USA).

Histologic analysis

A part of the kidney taken on day 6 was fixed with 4% paraformaldehyde, embedded in paraffin, and cut into 4- μm sections. These were stained with periodic acid–Schiff reagent (PAS). To assess tubule-interstitial injury, PAS-stained kidney sections were analyzed using a semi-quantitative grading as described previously (21). Apoptotic cell death was determined on the kidney sections (4- μm thick) by TUNEL staining using an *in situ* apoptosis detection Kit (Takara) as described elsewhere (21). Tubular cell proliferation was detected using anti-Ki67 Ab (Abcam, Cambridge, UK). To detect the endogenous level of endothelial nitric oxide (eNOS) protein, eNOS staining was also performed (Cell Signaling Technology, Beverly, MA, USA).

Determination of cytokine concentration in the rSVF-treated kidney

Kidney samples taken on day 6 were homogenized and centrifuged, and the supernatant collected. The

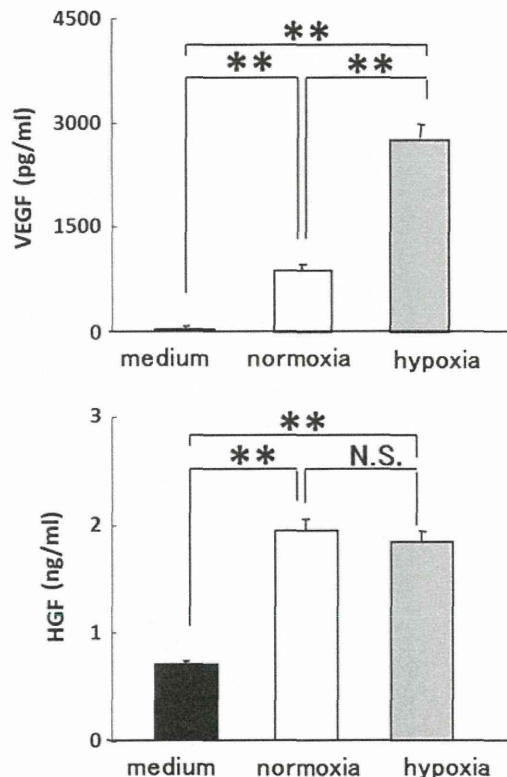


Figure 1. Cytokine production by hSVF cells. The levels of VEGF and HGF produced by hSVF cells were measured. The black bars show the basal levels in the culture medium. The white bars show the levels of cytokines produced by hSVF cells that were cultured under normoxic conditions. Gray bars show the cytokine levels from hSVF cells that were cultured under hypoxic (1% O_2) conditions. $**P < 0.01$ versus control medium.

levels of VEGF and HGF were determined using sandwich ELISA kits (Institute of Immunology Co. Ltd).

Rat experimental protocol 2: rSVF cell tracing study

To clarify whether rSVF cells had differentiated into renal cells, we performed a cell-tracking study. rSVF cells were labeled with Carboxy-fluorescein diacetate, succinimidyl ester, (Molecular Probes Inc., Eugene, Oregon, USA) (CFDA SE) (Invitrogen, CA, USA), and the labeled cells were injected into the renal subcapsules of rats ($n = 5$) 1 day after cisplatin injection. To the control rats ($n = 5$), saline was injected instead of rSVF cells. Rats were killed on day 14 and kidney samples taken for study. Frozen sections cut to 2- μ m thickness were stained with goat anti-rabbit angiotensin-converting enzyme (ACE) Ab (22), rabbit anti-rat VEGF (Lab Vision, Fremont, CA, USA)

or rabbit anti-rat HGF (Institute of Immunology Co. Ltd), followed by rhodamin-labeled rabbit anti-goat IgG Ab or goat anti-rabbit IgG Ab (Chemicon, Temecula, CA, USA).

Rat experimental protocol 3: i.p. administration of rSVF or conditioned media

A right heminephrectomy was performed on 8-week-old male F344 rats ($n = 18$). Seven days later (day 0), AKI was induced by s.c. injection of cisplatin (7 mg/kg). On day 1, 1×10^6 non-expanded SVF cells ($n = 6$), 24-h rSVF conditioned media or media only ($n = 6$) were injected into the peritoneal space. Blood samples were collected on days 0, 2, 4, 8 and 14, and the levels of serum creatinine were measured using a Daiya Auto Crea kit (Daiya Shiyaku).

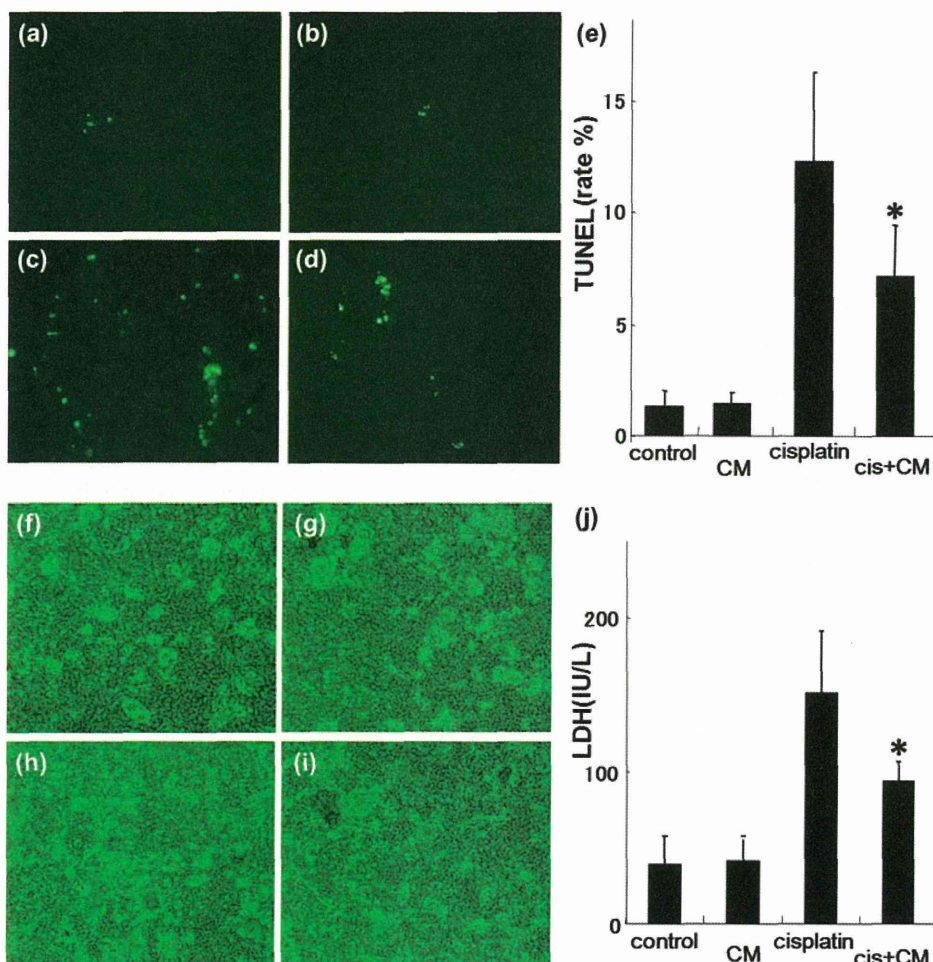


Figure 2. Effects of hSVF on tubular apoptosis and necrosis. TUNEL staining was performed on a primary culture of hRPTEC that had been cultured in control medium only (control) (a), conditioned medium of cells (CM) (b), control medium to which cisplatin has been added (cisplatin) (c) or hSVF-conditioned medium with cisplatin (CM + cisplatin) (d). (e) The rates of TUNEL-positive cells among the total hRPTEC cultured under each condition. (f-i) Representative bright-field images of hRPTEC in each condition. (j) Levels of LDH, a marker of necrosis, in the supernatant of hRPTEC. * $P < 0.05$ versus cisplatin.

Statistical analyses

Statistical analyses were performed using the software program Stat View 5.0 (SAS Institute, Cary, NC, USA). A Student's *t*-test was used to determine whether significant differences existed between the two groups. Two-way analysis of variance (ANOVA) was employed to determine whether there was a significant difference among three or four groups. When a statistical difference was indicated by ANOVA, further analysis was performed using Scheffe. Values of $P < 0.05$ were considered to be statistically significant. All values are expressed as mean \pm SD.

Results

Characterization of hSVF cells

One of the advantages of using adipose-derived cells for regenerative therapy is that fat contains a

relatively large number of stem/progenitor cells. The number of nucleate cells in SVF obtained from the liposuction aspirate was $1.63 \pm 0.40 \times 10^8/1$ L of adipose portion ($n = 9$). The number was consistent with previous studies (23). In order to characterize hSVF, cell-surface markers were examined. FACS analysis revealed that 39.6% of hSVF cells were positive for CD13, 19.9% for CD31, 37.0% for CD34, 36.6% for CD45 and 48.4% for CD90. These were comparable with the results of previous studies (24).

We studied the expression levels of VEGF and HGF, as these cytokines were secreted by adipose-derived MSC and promoted regeneration of the vessels (14). The results of immunoassays showed that hSVF cells secreted a significant amount of VEGF and HGF. Hypoxia further enhanced the level of VEGF ($P < 0.01$) but not the HGF level (Figure 1).

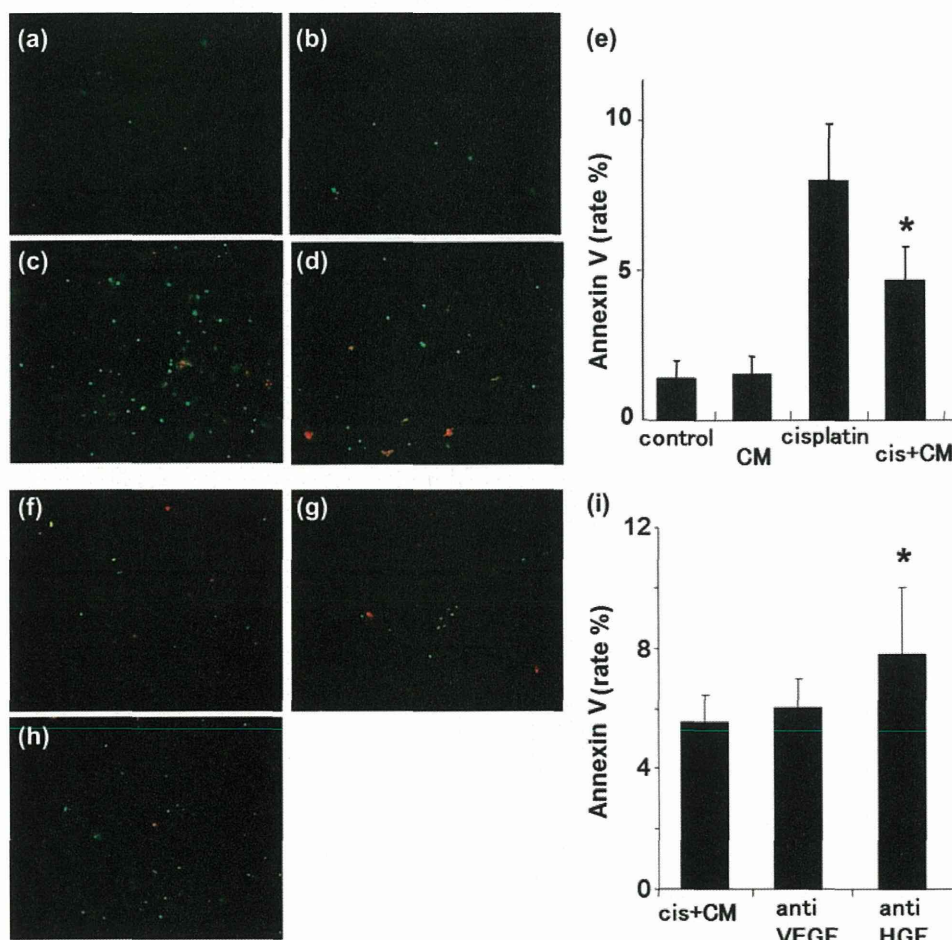


Figure 3. Effects of the cytokines secreted from hSVF cells on tubular cell apoptosis. Annexin V staining was performed on hRPTEC that had been cultured in control medium (control) (a), an hSVF-conditioned medium (CM) (b), control medium with cisplatin (cisplatin) (c) or an hSVF-conditioned medium with cisplatin (CM + cisplatin) (d). In the next experiment, hRPTEC were cultured in conditioned medium with cisplatin (CM + cisplatin) (f) and anti-VEGF Ab (g) or anti-HGF Ab (h) was added. (e, i) Rates of the Annexin V-positive cells measured by flow cytometry. * $P < 0.05$ versus cisplatin (e) or CM + cisplatin (f).

Anti-apoptotic effect of hSVF

The effects of cytokines secreted by hSVF were studied on hRPTEC. The number of TUNEL-positive cells increased when cisplatin was administered, suggesting apoptosis or necrosis had occurred. The conditioned medium from hSVF cell cultures suppressed the number of TUNEL-positive cells among hRPTEC ($P < 0.05$) (Figure 2a–e). The bright field images for each group are shown in Figure 2f–i. The conditioned medium from hSVF also decreased the

level of LDH released from hRPTEC, which is a marker of necrosis ($P < 0.05$) (Figure 2j).

Apoptosis in hRPTEC was quantified further by counting the Annexin V-positive cells using flow cytometry. Cisplatin increased the number of Annexin V-positive cells, and the conditioned medium from hSVF suppressed the apoptosis ($P < 0.05$) (Figure 3a–e). In order to clarify the mechanism, Ab against HGF and VEGF were applied to the hRPTEC culture. Anti-HGF Ab significantly suppressed the anti-apoptotic

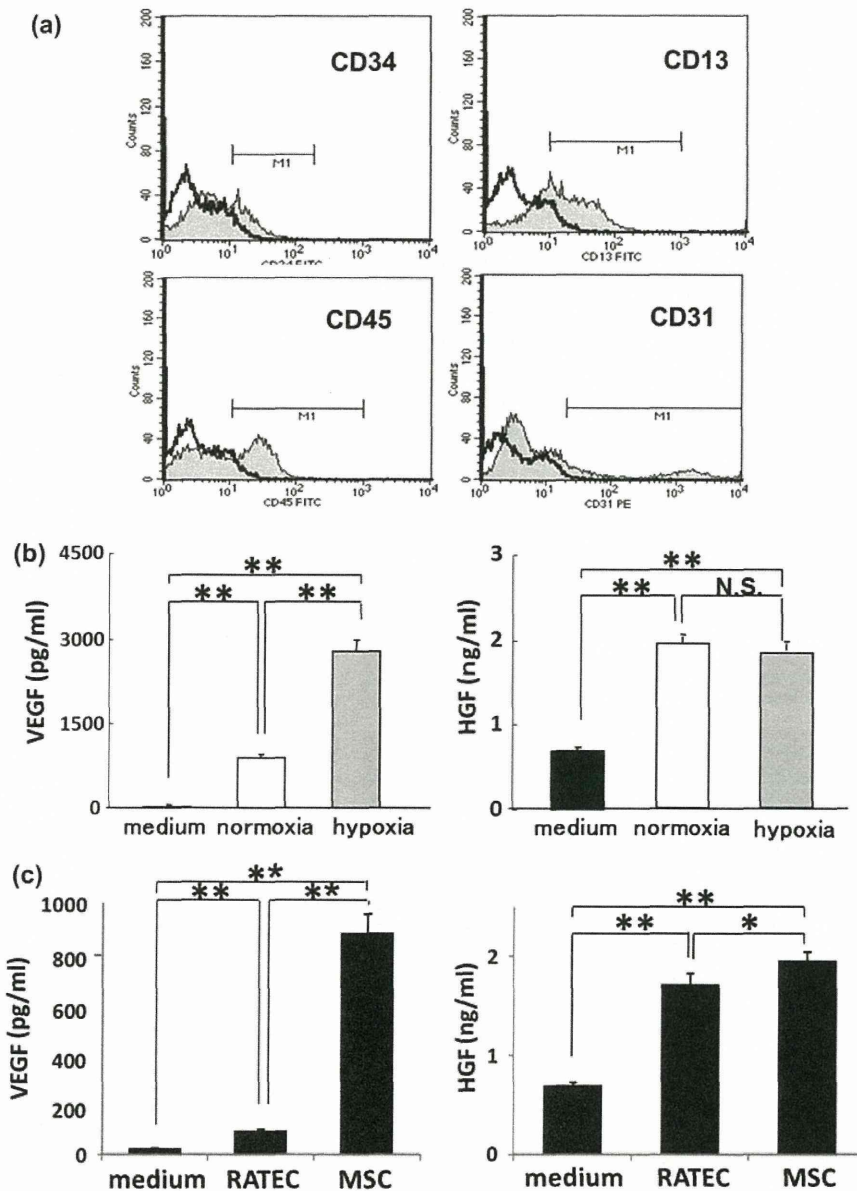


Figure 4. Characteristics of rSVF. (a) The cell-surface markers of rSVF cells. FACS analysis revealed that rSVF expressed CD34 (38.9%), CD13 (53.9%), CD45 (43.0%), and CD31 (16.5%). (b) The levels of VEGF and HGF produced by rSVF cells. Black bars show the basal levels in the culture medium. Blank bars show the levels of the cytokines secreted from rSVF cells that had been cultured under normoxic conditions. Gray bars show the levels of cytokines from rSVF cells that had been cultured under hypoxic (1% O₂) conditions. (c) The levels of VEGF and HGF produced by RATEC and MSC. * $P < 0.05$, ** $P < 0.01$.

for personal use only.

effects of hSVF ($P < 0.05$), whereas anti-VEGF Ab did not (Figure 3f–i).

Characterization of rSVF cells

We then studied the basic characteristics of rSVF taken from the subcutaneous adipose tissue, and the results were compared with those of humans. FACS analysis revealed rSVF cells expressed CD34 (38.9%), CD13 (53.9%), CD45 (43.0%) and CD31 (16.5%) (Figure 4a), similar to the results obtained in the experiments with hSVF cells. Moreover, rSVF cells secreted VEGF and HGF, and hypoxia enhanced the expression level of VEGF ($P < 0.01$) but not HGF (Figure 4b). These results were also consistent with those from the hSVF experiment (Figure 1).

As SVF are composed of heterogeneous cell populations, we then measured VEGF and HGF from MSC and RATEC to determine which cell type was responsible for secretion from SVF. MSC secreted more cytokines than RATEC, and the concentration of cytokines was similar to that of SVF (Figure 4c).

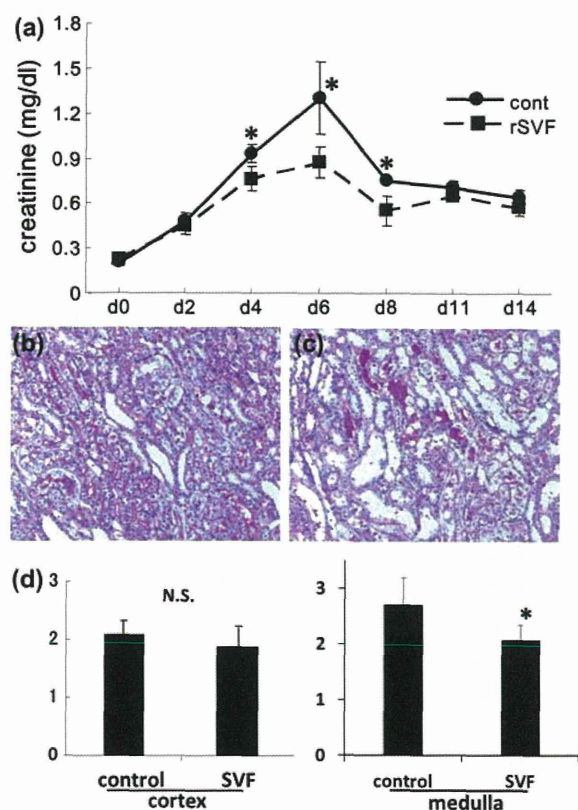


Figure 5. Effects of rSVF on renal function and histology in a rat AKI model induced with cisplatin. (a) The serum creatinine levels in the control rats (blue line) and rSVF-treated rats (pink line). (b, c) Outer medulla of the PAS-stained kidney section from control rats (b) and rSVF-treated rats (c). (d) Semi-quantitative scoring of the tubular damage in the cortex and medulla. Original magnification $\times 200$. * $P < 0.05$.

Effects of rSVF on renal function and histology in an AKI model

The therapeutic effects of rSVF were studied using a rat model of cisplatin-induced AKI. Transplantation of rSVF cells into the subcapsular space of the kidney on day 1 significantly suppressed the increase of creatinine levels on days 4, 6, 8 and 11 compared with the administration of medium only ($P < 0.05$) (Figure 5a). Examination of PAS-stained kidney sections on day 6 showed that tubular injury had occurred mainly in the outer medulla, but not in the cortex. A comparison between the control and rSVF groups revealed that SVF had greatly attenuated this tubular damage (Figure 5b,c). The severity of the tubular damage, including tubular dilatation, degeneration and cast formation, was scored. Administration of rSVF resulted in significantly better scores in the medulla than the control group ($P < 0.05$) (Figure 5d).

Direct visualization of the renal cortical capillaries

The effect of rSVF on renal blood flow was examined by analyzing direct images obtained with a CCD videomicroscope system on day 14. The movement of erythrocytes was observed in the cortical peritubular capillaries, and cortical blood flow speed was determined by an analysis of the speed of the erythrocytes. In the control group, the renal cortical peritubular capillaries shrank and blood flow was impeded (Figure 6a). In contrast, the capillaries were observed to be more dilated, and blood flowed faster and smoother, in the rSVF-treated rats (Figure 6b). The calculated blood flow velocity in the rSVF group was significantly faster than in the control group ($P < 0.05$) (Figure 6c). The renal cortical capillaries were stained with eNOS, and rSVF-treated capillaries were stained but not control capillaries (Figure 6d,e).

TUNEL assay of the kidney

The contribution of apoptosis and necrosis to the renoprotective properties of rSVF was assessed by performing a TUNEL assay on the kidney sections obtained on day 6. In the medium-treated rats, TUNEL-positive cells were localized mainly in the outer medulla. Transplantation of rSVF significantly decreased the number of TUNEL-positive cells in the medulla compared with medium only ($P < 0.05$) (Figure 7).

Cytokines in the kidney

As SVF cells produced significant levels of VEGF and HGF *in vitro*, we measured the concentrations of

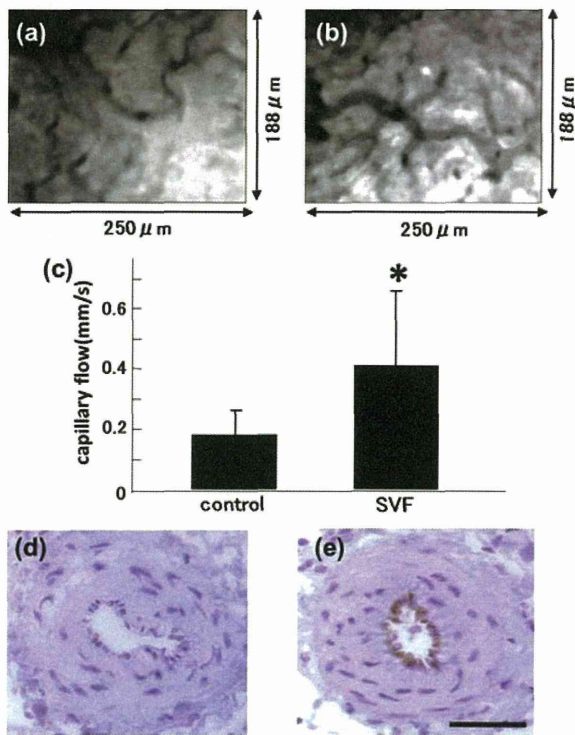


Figure 6. Direct visualization of the renal cortical blood flow. (a, b) Representative images of the renal cortical capillary of control rats (a) and rSVF-treated rats (b). (c) The velocity of the capillary blood flow. (d, e) eNOS staining was performed with renal cortical capillaries in both groups. * $P < 0.05$.

these two cytokines in the renal cortex and medulla on day 14 after cisplatin administration. The VEGF level was significantly higher in the cortex of the rSVF group than in the control group ($P < 0.01$), while no difference was observed in the medulla. In

contrast, the HGF level was significantly higher in both the cortex ($P < 0.05$) and medulla ($P < 0.01$) in the rSVF group than in the control (Figure 8a–d). The mitogenic effect was determined with Ki67 staining. Both the cortex and medulla in the rSVF group stained more Ki67-positive cells than the control group (Figure 8e–j).

Transplanted rSVF cells in the kidney

To investigate whether rSVF cells are directly or indirectly involved in kidney repair, we injected CFDA labeled-rSVF cells into the renal subcapsular space 1 day after cisplatin administration. Rats were killed on day 14 and kidney samples were obtained. Most of the cells positive for CFDA (green) remained alive in the subcapsules (Figure 9a–c). Occasionally a few rSVF cells were observed in the interstitium of the kidney, but those cells were not located in the tubular cell layer nor in the vascular cell layer. We found that strong staining for VEGF (red) was localized mainly around the CFDA-positive cells (green) in the subcapsules of the rSVF-treated rats, while no staining was observed in the control rats (Figure 9d,e). In contrast, strong staining of HGF (red) was localized in the subcapsules, and moderate expression was observed in the tubules of the medulla among the rSVF-treated rats whereas only weak staining was observed in the control rats (Figure 9f,g).

Intraperitoneal administration of rSVF cells or conditioned media

In order to study whether i.p. injection of rSVF is as effective as subcapsular administration, an additional

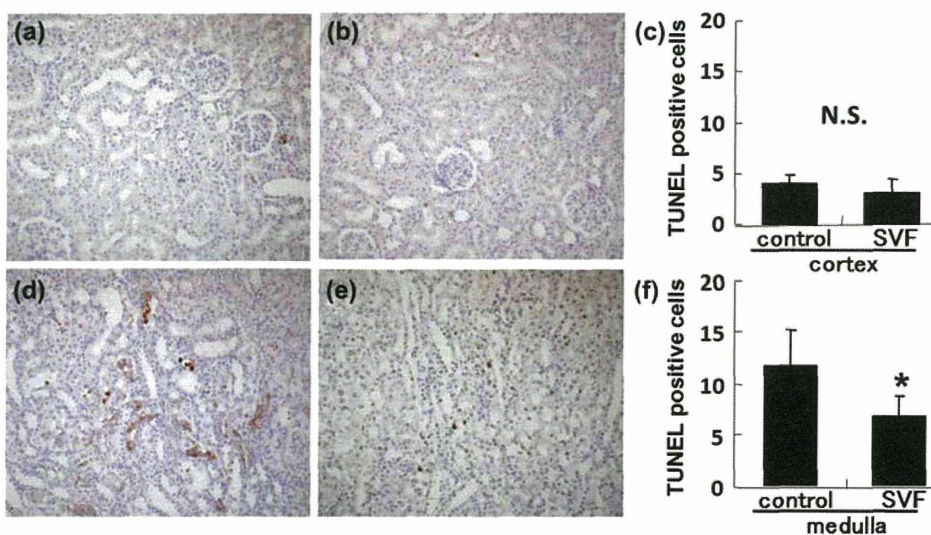


Figure 7. TUNEL staining of the kidney. (a, b, d, e) Representative photographs of TUNEL staining of the renal cortex (a, b) and medulla (d, e) are shown. A control medium (a, d) or rSVF (b, e) was administered to rats. (c, f) The rates of TUNEL-positive cells in the cortex (c) and medulla (f). Original magnification $\times 200$. * $P < 0.05$.

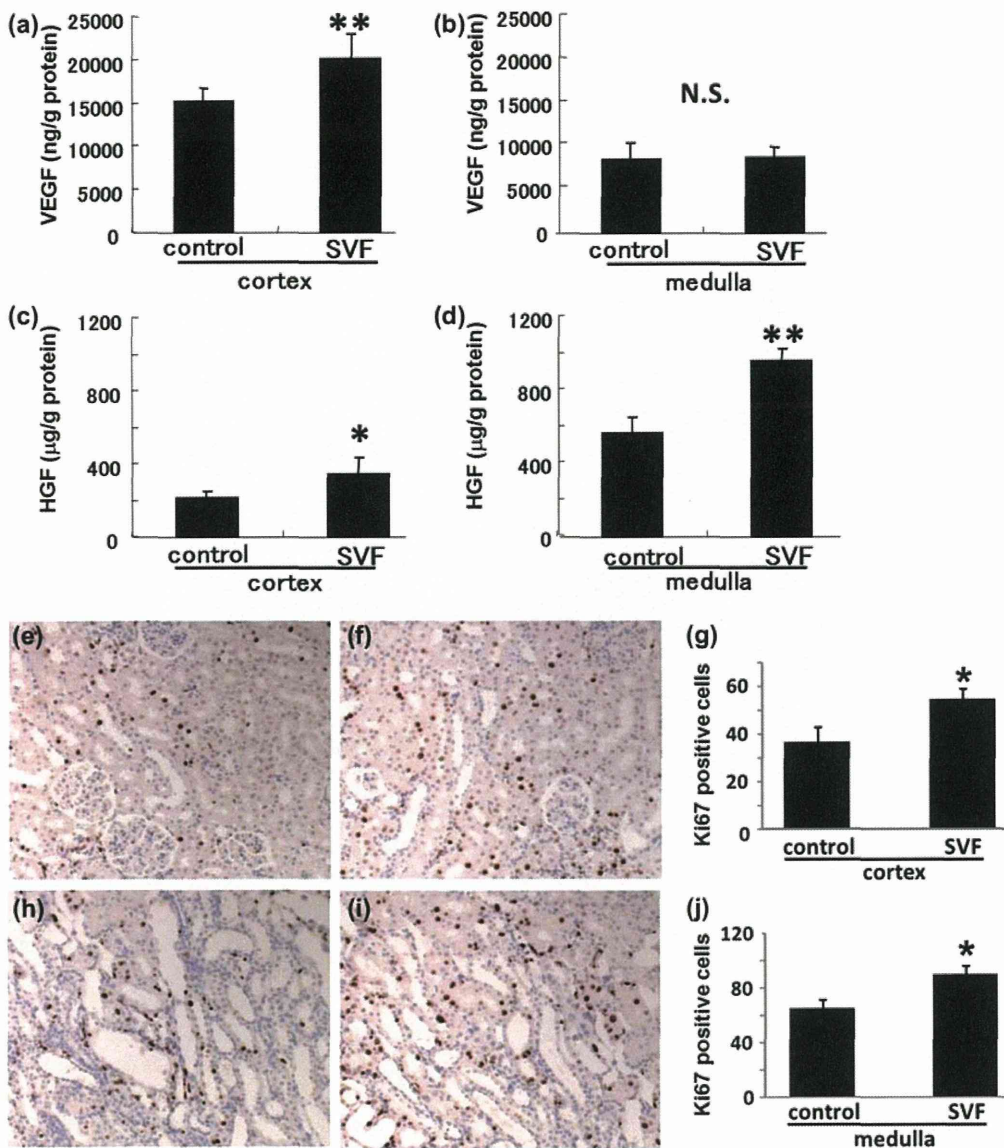


Figure 8. Cytokines and tubular cell proliferation in the kidney. (a–d) Cytokine concentrations in the homogenates of kidney samples taken from control rats and rSVF-transplanted rats on day 6 were measured. The levels of VEGF and HGF in the renal cortex or medulla are shown. (e, f, h, i) Representative photographs of Ki67 staining of the renal cortex (e, f) and medulla (h, i) are shown. A control medium (e, h) or rSVF (f, i) was administered to rats. (g, j) The rates of Ki67-positive cells in the cortex (g) and medulla (j). Original magnification $\times 400$. * $P < 0.05$, ** $P < 0.01$.

experiment was performed. AKI was induced in rats that were then given i.p. injections of rSVF cells, rSVF conditioned media (CM) or culture media only (control) on day 1. Creatinine levels were similar up to day 14 in all three groups (Figure 10).

Discussion

The data presented here show for the first time that non-expanded adipose-derived cells ameliorate AKI. Our results indicate that SVF cells exert their renoprotective activity via pro-angiogenic and mitogenic factors when administered into renal subcapsules.

Previous studies have demonstrated that MSC derived from BM contribute to tissue repair in damaged organs (25,26). Recent studies have shown that adipose tissue-derived MSC protect tissues from acute and chronic damage and accelerate regeneration in the heart, liver, brain and kidney (27–30). Kidney-derived MSC also promote functional recovery of an ischemic kidney (31). One of the limitations of using MSC in the clinical setting is that they must be expanded *in vitro* beforehand, a process that takes at least 2 weeks. In contrast, SVF can be used readily in patients without culturing. In our study, we obtained $1.0\text{--}2.0 \times 10^8$ cells, a number sufficient

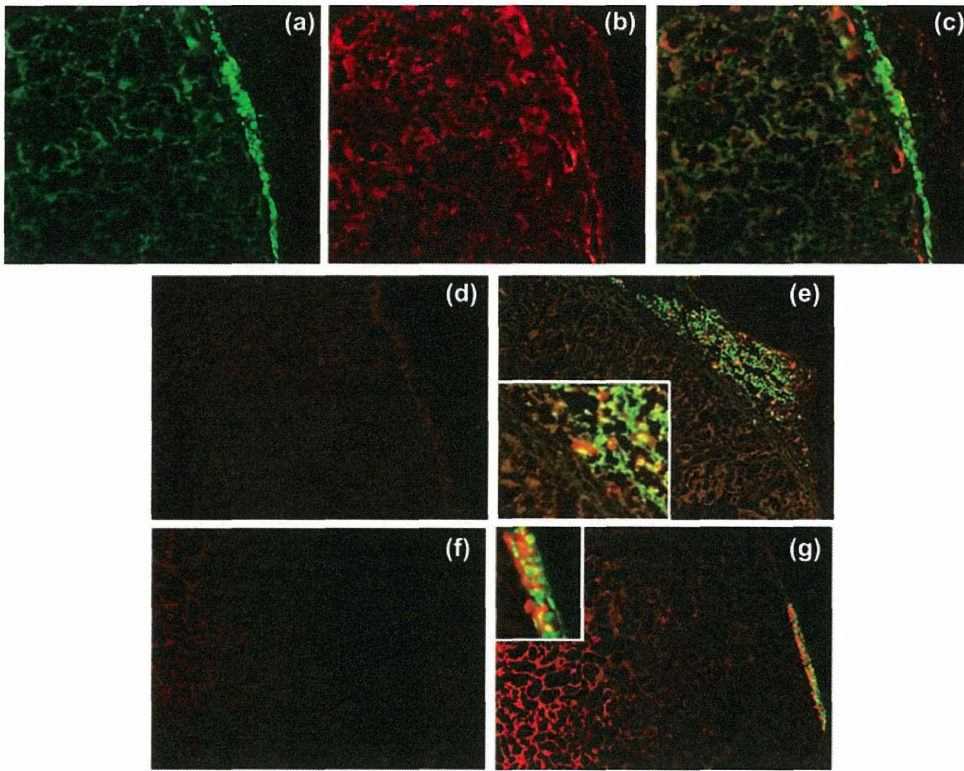


Figure 9. Transplanted rSVF cell trace and cytokine expression. (a, b, c, e, g) Representative photographs of the kidney to which rSVF cells labeled with CFDA (green) were injected 2 days after cisplatin administration. (d, f) Representative photographs of the control kidney to which medium only was administered on day 1 after cisplatin administration. The samples were taken on day 14. (a) rSVF cells (green) were detected in the surface of the kidney. (b) Proximal renal tubule cells were stained with anti-ACE Ab (red). (c) A merged photograph shows that rSVF cells were localized in the subcapsule of the kidney. (d, e) VEGF stained in red. (f, g) HGF stained in red. Original magnification $\times 100$.

for human therapy, from 1 L liposuction aspirate. Therefore SVF has a clear advantage over MSC, especially when applied to the treatment of acute diseases including AKI.

Our study shows that SVF cells produce a significant amount of VEGF *in vitro*. The level of VEGF was elevated in the renal cortex of rats that were given SVF, and strong VEGF staining was observed in the SVF cells. These results suggest that SVF cells produce VEGF *in vivo* after injection into the subcapsular space of the kidney. Direct visualization of the renal cortex revealed that the capillary blood flow speed increased in rats given SVF. The immunohistochemistry of the renal cortical capillaries showed the expression of endogenous eNOS in SVF-treated rats. VEGF is known to increase the eNOS level, which dilates the capillaries (32). Thus VEGF is one of the mediators by which SVF ameliorates AKI.

The present study also shows that SVF cells produce HGF *in vitro*. We found that SVF cell-producing factors limited tubular cell apoptosis and necrosis induced by cisplatin. Using neutralizing anti-HGF Ab, we showed that the anti-apoptotic effects of SVF

can be attributed in part to HGF. Our *in vivo* study demonstrated that apoptotic cell death was detected mainly in the outer medulla of rats injected with cisplatin, and SVF decreased this level. ELISA showed that the HGF concentration was higher in both the

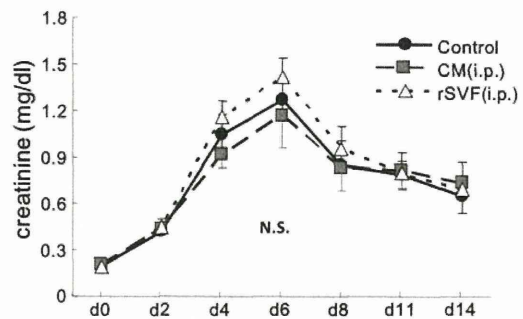


Figure 10. Intraperitoneal administration of rSVF cells or conditioned media. AKI was induced in rats with cisplatin 7 days after undergoing a right heminephrectomy (day 0). On day 1, rSVF cells (triangles), rSVF-conditioned media (CM) (squares) or culture media only (control) (circles) were injected i.p.. The graph shows serum creatinine levels in each group. No significant difference was observed at any point.

cortex and medulla. Immunostaining revealed that SVF cells were localized almost exclusively in the subcapsules and were producing HGF. Only a faint staining for HGF was observed in the tubular epithelial cells of the control rats, whereas the staining level in tubules of the medulla was significantly enhanced in rats injected with SVF. One possible explanation of this phenomenon is that the previous study shows that HGF promotes the expression level of HGF itself (33). Therefore it is likely that the HGF produced by SVF cells in our study promoted further HGF expression in the tubular cells, and thus attenuated the tubular injury. In addition, HGF is a potent proangiogenic and mitogenic factor, which limits renal injury by promoting renal capillary regeneration and proliferating renal tubular cells (8).

In our cell-tracking experiment, most of the SVF cells were still localized in the subcapsular space at 2 weeks after injection, and only a few cells could be detected inside the kidney. Even in such cases, SVF cells were not incorporated into the vessels or the tubules. In other words, no evidence of transdifferentiation was observed. These results are consistent with most of the recent studies using BM-derived MSC (26). We conclude here that the renoprotective properties of SVF are mediated mainly by paracrine mechanisms.

In this study, we first tried a method of subcapsular injection for the purpose of obtaining the maximum effect while using a limited number of SVF cells and avoiding the possible adverse effects of intravenous (i.v.) injection, such as pulmonary infarction. A previous study had shown that BM-derived MSC ameliorate AKI when given either i.v. or i.p. (30). This study also shows that even an i.v. injection of MSC-conditioned medium is as effective. We then performed i.p. administration of rSVF cells or rSVF-conditioned media on rat AKI and found that neither of these two showed any therapeutic effects on renal function. These results suggest that subcapsular injection is necessary when rSVF is used in treatment for kidney disease. In the clinical setting, this procedure can be done while the kidney is exposed during surgery. One of the possible applications of SVF is in kidney transplantation, especially when a marginal kidney is used. Another possible application of this cell therapy is for patients with small-size renal cell carcinoma. This condition requires a partial nephrectomy, during which the residual kidney is damaged by ischemia and reperfusion. We are currently preparing for a clinical trial to apply SVF to patients with this condition. In summary, our results demonstrate for the first time that the subcapsular administration of non-expanded adipose tissue-derived cells protects the kidney from acute injury and provides the basis for a novel therapeutic concept for renal disease.

Acknowledgments

The authors are indebted to Dr. Y. Kitagawa (Nagoya University, Nagoya) for providing cells used in these studies. And the authors also thank the excellent technical assistance of Ms Y. Sawa, N. Asano and Mr N. Suzuki.

Disclosure of interest: None declared.

References

- Asahara T, Murohara T, Sullivan A, Silver M, van der Zee R, Li T, et al. Isolation of putative progenitor endothelial cells for angiogenesis. *Science*. 1997;275:964–7.
- Rafii S, Lyden D. Therapeutic stem and progenitor cell transplantation for organ vascularization and regeneration. *Nat Med*. 2003;9:702–12.
- Goligorsky MS, Kuo MC, Patschan D, Verhaar MC. Review article. Endothelial progenitor cells in renal disease. *Nephrology (Carlton)*. 2009;14:291–7.
- Kamihata H, Matsubara H, Nishiue T, Fujiyama S, Tsutsumi Y, Ozono R, et al. Implantation of bone marrow mononuclear cells into ischemic myocardium enhances collateral perfusion and regional function via side supply of angioblasts, angiogenic ligands, and cytokines. *Circulation*. 2001;104:1046–52.
- Tateishi-Yuyama E, Matsubara H, Murohara T, Ikeda U, Shintani S, Masaki H, et al. Therapeutic angiogenesis for patients with limb ischaemia by autologous transplantation of bone-marrow cells: a pilot study and a randomised controlled trial. *Lancet*. 2002;360:427–35.
- Wollert KC, Meyer GP, Lotz J, Ringes-Lichtenberg S, Lippolt P, Breidenbach C, et al. Intracoronary autologous bone-marrow cell transfer after myocardial infarction: the BOOST randomised controlled clinical trial. *Lancet*. 2004;364:141–8.
- Fortuin FD, Vale P, Losordo DW, Symes J, DeLaria GA, Tyner JJ, et al. One-year follow-up of direct myocardial gene transfer of vascular endothelial growth factor-2 using naked plasmid deoxyribonucleic acid by way of thoracotomy in no-option patients. *Am J Cardiol*. 2003;92:436–9.
- Morishita R, Aoki M, Hashiya N, Makino H, Yamasaki K, Azuma J, et al. Safety evaluation of clinical gene therapy using hepatocyte growth factor to treat peripheral arterial disease. *Hypertension*. 2004;44:203–9.
- Henry TD, Annex BH, McKendall GR, Azrin MA, Lopez JJ, Giordano FJ, et al. The VIVA trial: Vascular endothelial growth factor in Ischemia for Vascular Angiogenesis. *Circulation*. 2003;107:1359–65.
- Kastrup J, Jorgensen E, Ruck A, Tagil K, Glogar D, Ruzyllo W, et al. Direct intramyocardial plasmid vascular endothelial growth factor-A165 gene therapy in patients with stable severe angina pectoris. A randomized double-blind placebo-controlled study: the Euroinject One trial. *J Am Coll Cardiol*. 2005;45:982–8.
- Zuk PA, Zhu M, Mizuno H, Huang J, Futrell JW, Katz AJ, et al. Multilineage cells from human adipose tissue: implications for cell-based therapies. *Tissue Eng*. 2001;7:211–28.
- Miranville A, Heeschen C, Sengenès C, Curat CA, Busse R, Bouloumié A. Improvement of postnatal neovascularization by human adipose tissue-derived stem cells. *Circulation*. 2004;110:349–55.
- Sanz-Ruiz R, Fernandez-Santos E, Dominguez-Munoz M, Parma R, Villa A, Fernandez L, et al. Early translation of adipose-derived cell therapy for cardiovascular disease. *Cell Transplant*. 2009;18:245–54.

14. Iwashima S, Ozaki T, Maruyama S, Saka Y, Kobori M, Omae K, et al. Novel culture system of mesenchymal stromal cells from human subcutaneous adipose tissue. *Stem Cells Dev.* 2009;18:533–43.
15. Di Rocco G, Iachininoto MG, Tritarelli A, Straino S, Zacheo A, Germani A, et al. Myogenic potential of adipose-tissue-derived cells. *J Cell Sci.* 2006;119:2945–52.
16. Schenke-Layland K, Strem BM, Jordan MC, Deemedio MT, Hedrick MH, Roos KP, et al. Adipose tissue-derived cells improve cardiac function following myocardial infarction. *J Surg Res.* 2009;153:217–23.
17. Hoogendoorn RJ, Lu ZF, Kroeze RJ, Bank RA, Wuisman PI, Helder MN. Adipose stem cells for intervertebral disc regeneration: current status and concepts for the future. *J Cell Mol Med.* 2008;12:2205–16.
18. Urahama Y, Ohsaki Y, Fujita Y, Maruyama S, Yuzawa Y, Matsuo S, et al. Lipid droplet-associated proteins protect renal tubular cells from fatty acid-induced apoptosis. *Am J Pathol.* 2008;173:1286–94.
19. Suzuki S, Maruyama S, Sato W, Morita Y, Sato F, Miki Y, et al. Geranylgeranylacetone ameliorates ischemic acute renal failure via induction of Hsp70. *Kidney Int.* 2005;67:2210–20.
20. Ozaki T, Anas C, Maruyama S, Yamamoto T, Yasuda K, Morita Y, et al. Intrarenal administration of recombinant human soluble thrombomodulin ameliorates ischaemic acute renal failure. *Nephrol Dial Transplant.* 2008;23:110–9.
21. Shimizu H, Maruyama S, Yuzawa Y, Kato T, Miki Y, Suzuki S, et al. Anti-monocyte chemoattractant protein-1 gene therapy attenuates renal injury induced by protein-overload proteinuria. *J Am Soc Nephrol.* 2003;14:1496–505.
22. Maruyama S, Cantu E 3rd, Demartino C, Vladutiu A, Caldwell PR, Wang CY, et al. Membranous glomerulonephritis induced in the pig by antibody to angiotensin-converting enzyme: considerations on its relevance to the pathogenesis of human idiopathic membranous glomerulonephritis. *J Am Soc Nephrol.* 1999;10:2102–8.
23. Ashjian PH, De Ugarte DA, Katz AJ, Hedrick MH. Lipoplasty: from body contouring to tissue engineering. *Aesthet Surg J.* 2002;22:121–7.
24. Yoshimura K, Shigeura T, Matsumoto D, Sato T, Takaki Y, Aiba-Kojima E, et al. Characterization of freshly isolated and cultured cells derived from the fatty and fluid portions of liposuction aspirates. *J Cell Physiol.* 2006;208:64–76.
25. Ohnishi S, Ohgushi H, Kitamura S, Nagaya N. Mesenchymal stem cells for the treatment of heart failure. *Int J Hematol.* 2007;86:17–21.
26. Humphreys BD, Bonventre JV. Mesenchymal stem cells in acute kidney injury. *Annu Rev Med.* 2008;59:311–25.
27. Nakagami H, Morishita R, Maeda K, Kikuchi Y, Ogihara T, Kaneda Y. Adipose tissue-derived stromal cells as a novel option for regenerative cell therapy. *J Atheroscler Thromb.* 2006;13:77–81.
28. Sgodda M, Aurich H, Kleist S, Aurich I, Konig S, Dollinger MM, et al. Hepatocyte differentiation of mesenchymal stem cells from rat peritoneal adipose tissue in vitro and in vivo. *Exp Cell Res.* 2007;313:2875–86.
29. Constantin G, Marconi S, Rossi B, Angiari S, Calderan L, Anghileri E, et al. Adipose-derived mesenchymal stem cells ameliorate chronic experimental autoimmune encephalomyelitis. *Stem Cells.* 2009;27:2624–2635.
30. Bi B, Schmitt R, Israilova M, Nishio H, Cantley LG. Stromal cells protect against acute tubular injury via an endocrine effect. *J Am Soc Nephrol.* 2007;18:2486–96.
31. Chen J, Park HC, Addabbo F, Ni J, Pelger E, Li H, et al. Kidney-derived mesenchymal stem cells contribute to vasculogenesis, angiogenesis and endothelial repair. *Kidney Int.* 2008;74:879–89.
32. Nakagawa T. Uncoupling of the VEGF-endothelial nitric oxide axis in diabetic nephropathy: an explanation for the paradoxical effects of VEGF in renal disease. *Am J Physiol Renal Physiol.* 2007;292:F1665–72.
33. Ueki T, Kaneda Y, Tsutsui H, Nakanishi K, Sawa Y, Morishita R, et al. Hepatocyte growth factor gene therapy of liver cirrhosis in rats. *Nat Med.* 1999;5:226–30.

Antethoracic Pedicled Jejunum Reconstruction with the Supercharge Technique for Esophageal Cancer

Naoki Iwata · Masahiko Koike · Yuzuru Kamei · Chie Tanaka · Norifumi Ohashi · Goro Nakayama · Shuji Nomoto · Tsutomu Fujii · Hiroyuki Sugimoto · Michitaka Fujiwara · Yasuhiro Kodera

Published online: 7 August 2012
© Société Internationale de Chirurgie 2012

Abstract

Background Gastric tube is the first choice as an esophageal substitute for reconstruction after esophagectomy. Colon or jejunum is selected for patients in whom stomach cannot be used. Colon interposition is reported to have a high incidence of anastomotic leakage and mortality. For safer surgical treatment, the authors adopted supercharged pedicle jejunum reconstruction as the operation of choice in patients with esophageal cancer who had no stomach to use as an esophageal substitute. The aim of this study was to review our experience with this technique.

Methods From 2003 to 2009, esophagectomy and antethoracic pedicled jejunum reconstruction with the supercharge technique was performed in 27 patients with esophageal cancer at the Department of Gastroenterological Surgery (Surgery II), Nagoya University Hospital. Medical records of these 27 patients were retrospectively reviewed to determine demographic data, diagnosis, functional results, and perioperative course.

Results Median operating time, blood loss, hospital stay, and duration of enteral feeding were 636 min (range 454–856 min), 580 ml (range 208–1959 ml), 27 days (range 16–72 days), and 80 days (range 26–1740 days), respectively. There were no in-hospital deaths. Anastomotic

leakage occurred in two patients and was successfully managed conservatively. In 2 of 27 patients, the pedicled jejunum was of insufficient length, and additional procedures were needed to complete the anastomosis.

Conclusions Although antethoracic pedicled jejunum reconstruction with the supercharge technique is technically demanding, it is a reliable technique and contributes to successful reconstruction after esophagectomy for patients in whom stomach is not available for reconstruction.

Introduction

Gastric tube is the first choice as an esophageal substitute for reconstruction after esophagectomy for esophageal cancer. Colon or jejunum is selected for patients in whom stomach cannot be used for reconstruction because of prior gastrectomy or diagnosis of concomitant gastric cancer [1]. According to a national cancer registry in Japan, reconstructions using the colon and jejunum amounted to 4.9 and 4.2 %, respectively, of all esophageal cancer operations [2]. Esophageal reconstruction with organs other than the stomach is complicated and technically demanding. Nevertheless, the prognosis for patients with esophageal cancer with a history of gastrectomy is not inferior to that of patients without such history, and a similar treatment strategy should be offered to these patients [3].

Reconstruction by colonic interposition is widely accepted as an alternative in such cases [1, 4, 5]. However, this procedure has been associated with high incidences of anastomotic leakage and mortality [5–10]. Moreover, the procedure is associated with various shortcomings such as concerns regarding insufficient blood supply to the colonic segment because of anatomic variety or arteriosclerosis of the feeding arteries, the need for three gastrointestinal anastomoses, and carcinogenesis of the colonic segment used for reconstruction.

N. Iwata (✉) · M. Koike · C. Tanaka · N. Ohashi · G. Nakayama · S. Nomoto · T. Fujii · H. Sugimoto · M. Fujiwara · Y. Kodera

Department of Gastroenterological Surgery (Surgery II), Nagoya University Graduate School of Medicine, 65 Tsurumai-cho, Showa-ku, Nagoya, Aichi 466-8550, Japan
e-mail: iwt-nk@med.nagoya-u.ac.jp

Y. Kamei
Department of Plastic and Reconstructive Surgery, Nagoya University Graduate School of Medicine, 65 Tsurumai-cho, Showa-ku, Nagoya, Aichi 466-8550, Japan

On the other hand, reconstruction with jejunum has an inherent weakness in the limited access to the upper thorax for anatomic reasons. However, jejunum provides good motility, is less vulnerable to ischemia, has a diameter similar to that of the esophagus, and is rarely prone to carcinogenesis. The supercharge technique, done by anastomosing dissected jejunal vessels of the pedicle to their counterparts in the thoracic or cervical regions is therefore a compelling solution to the anatomic problem [11].

In 2003, to avoid the high mortality rate reported for colonic interposition and to solve the weakness inherent to the conventional jejunum reconstruction, we decided to adopt antethoracic pedicled jejunum reconstruction with the supercharge technique as the first choice of treatment for esophageal cancer patients in whom stomach cannot be used for reconstruction. The current study was conducted to review the outcomes of using this technique, including symptoms and eating habit during a follow-up of more than 1 year postoperatively.

Patients and methods

A total of 254 patients underwent esophageal ablation and reconstruction for esophageal cancer from 2003 to 2009 at the Department of Gastroenterological Surgery (Surgery II), Nagoya University Hospital, and antethoracic pedicled jejunum reconstruction with the supercharge technique was performed in 27 patients. The medical records of these 27 patients were reviewed retrospectively to evaluate the demographic data, diagnosis, functional results, and perioperative course. The median follow-up time among ongoing survivors was 1,250 days (range 480–2250 days).

Clinical staging of tumors was performed according to the tumor-node-metastasis (TNM) classification system, 6th edition, of the International Union against cancer [12].

Patients were diagnosed as having anastomotic stenosis when balloon dilatation had to be performed. The balloon dilatation was conducted when an endoscope 1 cm in diameter could not pass through the stenotic site. Anastomotic leakage was diagnosed by clinical findings or esophagography performed on postoperative day (POD) 7. To evaluate functional aspects of the reconstruction method, we examined the medical records for complaints regarding dysphagia, reflux, and diarrhea/abdominal pain suggestive of the dumping syndrome. The duration of enteral feeding was calculated to evaluate their eating habits.

Surgical technique

First, 26 of 27 patients underwent right thoracotomy, and esophagectomy was conducted in the left lateral decubitus position. The other patient underwent transhiatal

esophagectomy. Systematic lymph node dissection was invariably performed. Three-field lymph node dissection was performed when lymph node metastasis along the recurrent nerves was highly suspected by the preoperative imaging studies or detected intraoperatively by frozen sections. Subsequently, in supine position with extension of the neck, the collar and chest incisions were undertaken; laparotomy was performed with a median or transverse incision for prior gastrectomy patients. A skin flap of the chest wall was created as far as the medioclavicular line by dissecting along the fascia of the greater pectoral muscle to accommodate the jejunum that was to be used for reconstruction.

In the abdomen, the xiphoid process was removed and the area was covered with the peritoneum to avoid mechanical damage to the jejunum that had to be pulled up. Total gastrectomy with lymph node dissection based on the Japanese Classification of Gastric Carcinoma [13] was performed in patients with concomitant gastric cancer. The remnant stomach was removed in patients with a history of distal gastrectomy.

The key to the success of this procedure was to mobilize the jejunum sufficiently so the vessels to be used for anastomosis could be placed as proximally as possible. Hence, the jejunum was dissected at about 10 cm from the ligament of Treitz, preserving the first branch vessel. We commonly used this first branch vessel as a donor vessel (Fig. 1). Purstring 45 (Covidien, Mansfield, MA, USA) was routinely used to thread the cervical esophagus for insertion and fixation of the anvil head, and esophagojejunosomy was performed using a circular stapler.

After the end-to-side esophagojejunal anastomosis, the blind end of the jejunum was closed 2 cm away from anastomosis because we were concerned that too large a

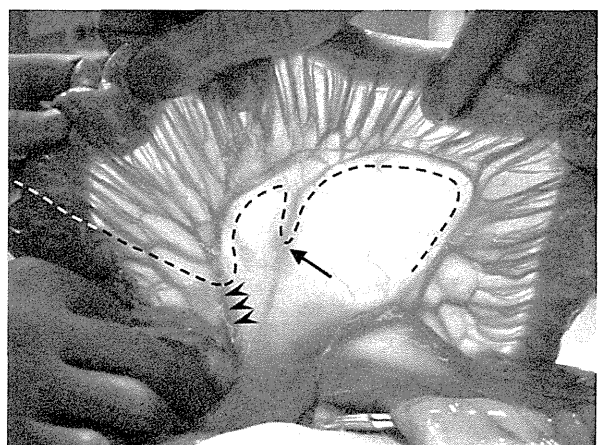
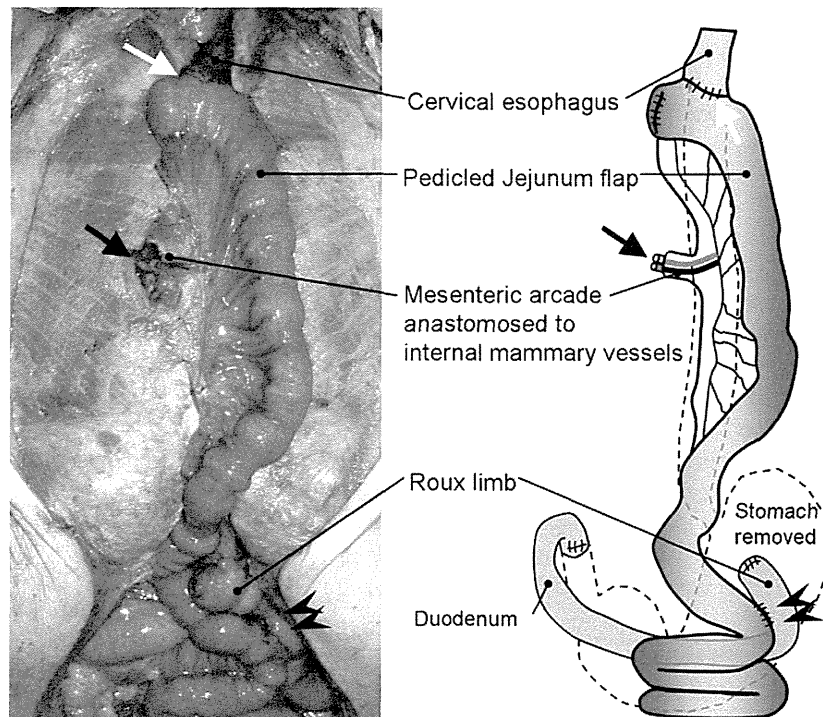


Fig. 1 First branch of the jejunal artery used as the donor vessel (arrowheads) and the ligated second jejunal vessel (arrow). Dashed line: cutting line of the mesentery

Fig. 2 Intraoperative photograph (left) and schema after reconstruction (right). Note the donor vessel (black arrow), esophagojejunal anastomosis (white arrow), and Roux-en-Y anastomosis (arrowheads)



blind end might result in pooling of ingested substances, leading to aspiration. After removing the third rib cartilage, the right internal mammary artery and vein were isolated for microvascular anastomosis. Revascularization was performed by a plastic surgeon (Y. K.) usually with the GEM microvascular anastomotic system (Synovis, Birmingham, AL, USA) for venous anastomosis and with 10-0 nylon interrupted sutures for arterial anastomosis. Because avoidance of excessive vascular flexure is considered the key to preventing formation of blood clots after revascularization, we performed esophagojejunostomy first and confirmed the position of jejunal vessels to be used for the anastomosis prior to the vascular reconstruction. Pulsation of the arcade and marginal arteries, the color of the flap, and peristalsis of the flap were observed closely during surgery. To avoid jejunal stasis, the jejunum used for the reconstruction was placed straight and fixed circumferentially at the orifice of the abdominal wall to avoid further jejunum from entering the subcutaneous cavity via peristalsis.

The reconstruction was completed by an abdominal Roux-en-Y anastomosis (Fig. 2). A tube jejunostomy using the STJ kit (Nipro, Osaka, Japan) was routinely placed in all patients for early nutritional support. At the end of the surgery, tension suturing between subcutaneous tissue and fascia of the greater pectoral muscle was performed so the skin did not compress the underlying jejunal pedicle. The chest wall was closed loosely, creating a partial skin

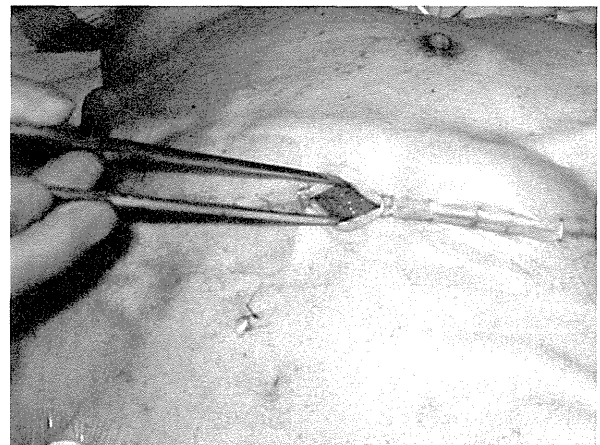


Fig. 3 Skin opening for checking on the color of the jejunal wall

opening above the pedicle so that, whenever deemed necessary, the color of the jejunum could be checked postoperatively (Fig. 3).

Postoperative care

Patients recovered in the intensive care unit under mechanical ventilation from which they were usually weaned late at night or on the day after surgery. Enteral feeding was started on POD 1. Contrast-enhanced esophagography was routinely performed on the POD 7 before

oral intake was initiated to ascertain that there was no evidence of anastomotic leakage or aspiration. After confirmation, the patient was started on semisolid meals. If they do not show difficulty swallowing, a regular diet was provided.

Results

During the 7-year period, 27 patients with esophageal cancer underwent esophagectomy with antethoracic pedicled jejunum reconstruction using the supercharge technique. Patient demographics and the reasons for utilizing this method of reconstruction and co-morbidities are listed in Tables 1 and 2, respectively. All patients had squamous cell carcinoma. The reasons for prior gastrectomy in 21 patients were for peptic ulcer in 12, gastric cancer in 7, and other causes in 2. The type of reconstruction after gastrectomy was Billroth type I in 15, Billroth type II in 5, and Roux-en-Y in 1.

Table 1 Demographics of 27 patients

Parameter	Data
Sex (M:F)	26:1
Age (years)	63 (54–77)
BMI (kg/m ²)	20.4 (15.2–24.3)
pTNM stage	
I	11 (41 %)
II	8 (29 %)
III	4 (15 %)
IV	4 (15 %)
Tumor location	
Cervical	2 (7 %)
Upper thoracic	3 (11 %)
Middle thoracic	17 (63 %)
Lower thoracic	5 (19 %)
Preoperative therapy	
None	18 (66 %)
Chemotherapy	4 (15 %)
Chemoradiotherapy	5 (19 %)
Radiotherapy	0
Co-morbidities	
Diabetes	5 (19 %)
Hypertension	3 (11 %)
Cerebral infarction	1 (4 %)
Old cardiac infarction	1 (4 %)
Tuberculosis	1 (4 %)
Liver cirrhosis	1 (4 %)
Renal sclerosis	1 (4 %)

Results are the median and range or the number and percent
BMI body mass index

Operative results, including duration of enteral feeding and perioperative complications, are presented in Table 3. The median operating time was 10.5 h, and median blood loss was 580 ml. Two patients underwent simultaneous laryngectomy because of concomitant laryngeal cancer in one and invasion of the esophageal cancer to the thyroid and larynx in the other. In 2 of the 27 patients, the jejunum did not reach the cervical esophagus. Division of the arcade vessel in the mesentery resulted in sufficient elongation of the jejunum for anastomosis in one of the patients (Fig. 4), and the other patient required additional free jejunum graft with vascular reconstruction between the cervical esophagus and pedicled jejunum (Fig. 5). Two patients developed anastomotic leakage, which healed with conservative treatment. One patient who underwent simultaneous laryngectomy for

Table 2 Reasons for not using a gastric conduit (*n* = 27)

Reason	No.
Prior gastrectomy	21 (78 %)
Concomitant gastric cancer	5 (19 %)
Prior abdominal trauma	1 (3 %)

Table 3 Operative outcome and complications

Outcome	No.
Mortality	
30-Day	0
In-hospital	0
Esophageal remnant necrosis	0
Reoperation	1 (4 %)
Operating time (min)	636 (454–856)
Operative blood loss (ml)	580 (208–1959)
Postoperative hospital stay (days)	35 (16–72)
Duration of enteral feeding usage (days)	80 (26–1740)
Removal date of jejunostomy tube	
Before discharge	4 (14 %)
≤3 months	13 (48 %)
3–6 months	5 (19 %)
>6 months	4 (15 %)
Unknown	1 (4 %)
Postoperative complications	
Anastomotic leakage	2 (7 %)
Pulmonary complication	2 (7 %)
Catheter-related sepsis	2 (7 %)
Anastomotic stenosis	1 (4 %)
Obstruction of pedicled jejunum	1 (4 %)
Ascitic fluid	1 (4 %)
Trachea necrosis	1 (4 %)

Results are the median and range, the number and percent, or as otherwise stated

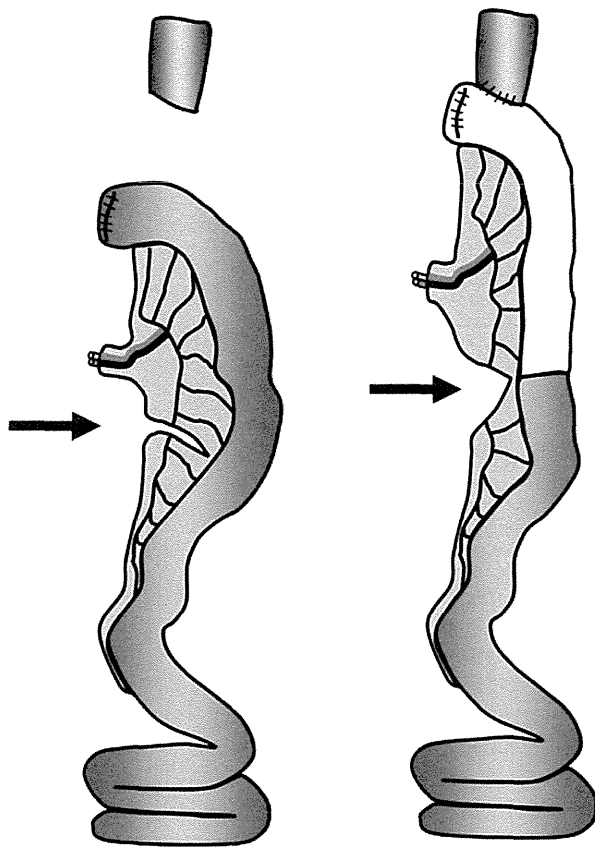


Fig. 4 Schema shows how to elongate the pedicled jejunum by dividing the arcade vessels (*black arrows*). *Light portion* (jejunum) represents the area to which the donor vessels supply blood

concomitant laryngeal cancer developed necrosis of the trachea that required reoperation.

Of the 27 patients, 26 tolerated a normal diet when they were discharged from the hospital, although tube feeding was also needed for nutritional support in 23 of the 27 patients. The jejunostomy tube was thus removed before discharge day in 4 patients. One other patient left the hospital without any oral intake because of anastomotic leakage but resumed oral feeding 1 month after the discharge. None of the 27 patients complained or showed signs of difficulty when swallowing, allowing the patients to eat a regular diet soon after their initial attempts with semisolid food.

One patient visited the outpatient clinic several times during the first 2 years after operation because of mechanical obstruction of the jejunum caused by adhesion; it was easily managed with conservative treatment. At 3 months after the operation, four patients complained at the outpatient clinic that they experienced occasional mild dysphagia, one of whom had delayed stenosis at the site of the anastomosis and underwent balloon dilatation 10 months after operation. Another two patients had mild

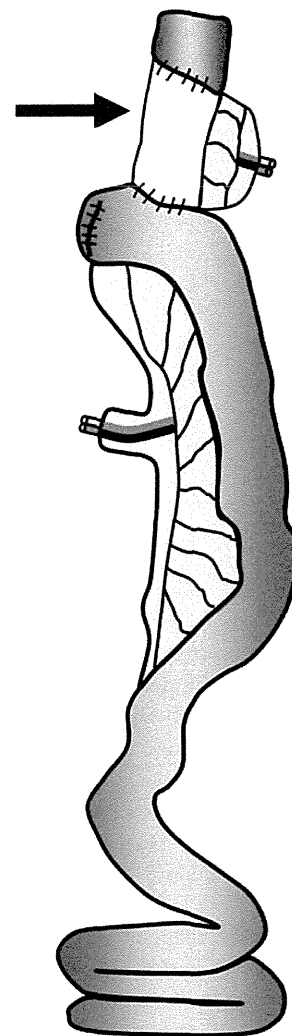


Fig. 5 Schema shows how the free jejunum graft was added (*black arrow*)

diarrhea and abdominal pain, indicating the dumping syndrome, which resolved through improved eating habits. At 1 year after the operation, 2 of the 27 patients had died. The remaining 25 patients were able to take a normal diet and nobody complained of dysphasia or symptoms suspicious of dumping syndrome. Currently, at a median follow-up time of 1,250 days (range 480–2252 days) or until death, five patients died of esophageal cancer and four more died of other diseases. In all, 18 are still alive.

Discussion

Patients with esophageal cancer in whom stomach is not available for reconstruction owing to their history of gastrectomy or coincidence of gastric disorder are likely to increase in countries where gastric cancer is not necessarily

Table 4 Articles describing jejunum reconstruction with the supercharge technique

Study	Year	No. of patients	Reconstruction route			30-Day mortality (%)	Necrosis (%)	Leakage (%)
			Subcutaneous	Retrosternal	Retrocardiac			
Longmire [18]	1947	1	1	0	0	0	0	NA
Androsov [19]	1956	11	11	0	0	0	9.1	NA
Hirabayashi [11]	1993	14	14	0	0	0	0	14.3
Heitmiller [23]	2000	1	0	1	0	0	0	0
Chana [25]	2002	11	11	0	0	0	0	36.4
Ascioti [17]	2005	26	0	13	13	0	7.7	19.2
Ueda [26]	2007	27	27	0	0	0	0	11.1
Doki [16]	2008	25	25	0	0	0	0	24.0
Barzin [24]	2011	5	0	5	0	0	0	20.0
Poh [22]	2011	51	0	31	20	0	5.9	20.0
Iwata (present)		27	27	0	0	0	0	7.4

NA not assessed

a fatal disease [3]. The surgical procedure to treat these patients is complicated and technically demanding [3]. The outcomes of gastrectomized esophageal cancer patients, however, depend on the clinical stages and are not necessarily inferior to those of nongastrectomized patients. Esophageal surgeons therefore need to establish a safer surgical procedure for esophageal patients in whom stomach is unavailable for reconstruction.

Colonic interposition has been the first choice for such cases [14], but this procedure has several shortcomings. The most serious problem is the high mortality rate, which was reported to be in the range of 3–29 % [5, 6, 8, 9] up to 2000. The mortality rate is decreasing [10]. In fact, many reports more recently have demonstrated the safety of colonic interposition [14, 15], although necrosis of esophageal remnant or anastomotic leakage would still lead to serious consequences. The postoperative hospital stay is longer with colon interposition than jejunal reconstruction when anastomotic leakage occurs [16], possibly because of the intestinal flora [16].

Because of anatomic limitations of the jejunum, pedicled jejunum reconstruction had been adapted to address disease in the lower esophagus. The advantages of this procedure are that the diameter of the jejunum is similar to that of the esophagus, peristalsis is abundant, it is free from intrinsic disease [17], and it has long-term durability. That only two anastomosis sites (esophagojejunal and Roux-Y anastomosis) are required for this procedure is also an advantage. Longmire reported pedicled jejunum reconstruction with the supercharge technique to make a long-segment jejunal flap and avoid ischemia of the flap [18]. In 1956, Androsov et al. [19] reported the benefit of this vascular anastomosis in esophageal reconstruction. In recent days, refinement of microsurgery has increased the average patency rate of anastomosed vessels to 95 % [20,

21]. Microvascular augmentation of the pedicled jejunum allows creation of a long conduit, and reconstruction not only for subtotal esophagectomy [11] but also for total esophagectomy [17] has been reported. As shown in Table 4, all reports that focused on esophageal reconstruction using a supercharged jejunum flap showed excellent results, with no 30-day mortality, apart from Poh et al. [22] who reported two in-hospital deaths.

Meticulous designing and simulation of the reconstruction is required to obtain sufficient length of the pedicled jejunum. Despite great efforts, there are times when it is not possible for the pedicled jejunum to reach the esophageal remnant during the operation. Harvesting a sufficient jejunal flap is reported to be difficult when the mesenterium is fatty and short with sparse collaterals [4]. In our series, alterations in the surgical procedure were required in two cases. In one case, excessive fat in the mesentery interfered with reconstruction, and the donor vessel could not reach the third rib cartilage. As a result, a marginal artery needed to be sacrificed to elongate the pedicled jejunum (Fig. 4). In another case, the primary cancer was located in the cervical esophagus, calling for simultaneous laryngectomy. Although the donor vessels reached the third rib cartilage, the remnant esophagus was too short for the jejunal pedicle to undergo anastomosis. The authors decided at this time to add another free jejunum graft for reconstruction (Fig. 5). Because this complex, time-consuming procedure requires additional gastrointestinal and vessel anastomoses, however, sacrificing the marginal artery should be considered the procedure of choice whenever it provides sufficient elongation of the jejunal pedicle for anastomosis.

Regarding the reconstruction route, the retrosternal route is usually shorter than the antethoracic route, but the esophageal remnant could in this case be compressed by the manubrium of the sternum, inducing congestion [10].